Mechanism of thermal entrainment of the circadian clock by newly identified post-transcriptional regulation

（新規転写後調節機構による体内時計の温度サイクルへの位相適応メカニズム）

2022

井ノ上　雄一

Contents

Introduction

Recent genome-wide transcriptome and proteome studies have revealed that mRNA expression levels only explain approximately 40% of the variation of protein product levels in cells, suggesting a potential importance of changeable protein production efficiency. Translation has long been considered as a static process, like a conveyor belt, but recent studies pointed to its variable nature[1]. Translation is not just a linear bridge between mRNA and protein, but is highly variable and characterized by a wide dynamic range (1,000 times that of transcription), local control within the cell, and reactions that consume up to 50% of the energy in the cell. These features suggest that translation may serve as a platform for parametric regulation of gene product expression. Upstream open reading frame (uORF) is short open reading frame whose start codon is located in the 5′ untranslated region (5′ UTR) of mRNA[2-4]. uORFs have been related to the regulation of protein expression of stress-related genes, such as ATF4[5]. However, the mechanisms underlying uORF-dependent regulation of translation efficiency are only limitedly understood. Especially, its physiological significance under non-stress condition is completely unknown.

The 24-hour rotation of the Earth creates temporal changes in the environment, forcing the organisms to acquire the ability to adapt to recurrent, thus anticipatable environmental changes[6]. A variety of physiological phenomena, such as thermogenesis and sleep-wake

cycles, have been identified to exhibit daily fluctuation[7]. Body temperature of thermostatic animals does not stay constant but displays a regular circadian fluctuation, which has an important physiological role in maintaining homeostasis of sleep and metabolism as well as entraining the peripheral circadian clocks in the body. Indeed, a subtle circadian fluctuation in body temperature within a physiologic range *in vivo* (35°C to 38.5°C in mice) has the ability to adjust or entrain the phase of the circadian clock in cultured cells[8, 9]. Although some of the heat or cold stress-related molecular regulators, such as the heat shock factor 1 and cold-inducible RNA-binding protein, are reported to participate in this entrainment mechanism[10-12], the precise mechanism(s) by which the physiological body temperature fluctuation affects the oscillation of the molecular clock in cells have remained unclear. One of the reasons for this unclarity is that most of previous studies have mainly focused on the contribution of mRNA regulation and paid less attention to protein translation in the control of the circadian clock.

In this research background and framework, I found that a mild increase in temperature in a physiological range (warming temperature shift, WTS) induced a ribosomal accumulation at the uORF region of *Per2* in cultured cells **(Chapter 1)**. WTS led to increased Per2 protein expression, which is regulated at a translational level in a uORF-dependent manner **(Chapter 2)**. To investigate the molecular mechanism underlying the temperature response of Per2 protein expression, I performed chemical library screening and revealed that blocking PI3K abrogated WTS-dependent Per2 protein accumulation **(Chapter 3)**. Finally, I showed that

PI3K and *Per2* uORF have a significant contribution to the establishment of the temperature entrainment of the circadian clock **(Chapter 4)**.

Methods

Temperature control

WTS was applied to cells by transferring the cell dish from a 35°C incubator to a 38.5°C-prewarmed incubator. The temperature of the medium was measured using an electronic thermometer and verified to approach 38.5°C by about 7−8 min after the transfer. Application of simulated body temperature was performed using a custom-modified convection-ventilated incubator box, in which temperature was controlled by peltier device and forced air circulation. This device allows the programming and recording of temperature profiles in real time with an accuracy of 0.1°C.

Ribo-seq and RNA-seq analysis

I used Dex-synchronized MEF cells treated with or without WTS for 2 h. Cells were lysed with a buffer containing 20 mM Tris-HCl [pH 7.5], 150 mM NaCl, 5 mM $MgCl_2$, 1 mM DTT, 1% Triton X-100, and 100 μg mL^{-1} cycloheximide (CHX). Following digestion of genomic DNA with DNase I (~25 U mL^{-1}, Thermo Fisher Scientific), the lysates were centrifuged at 20,000 × *g* and the resultant supernatant was processed for library generation. For Ribo-seq, samples (10 μg RNA each) were digested with 20 U RNase (Epicentre) at 25°C for 45 min, and the RNA fragments protected by ribosomes ranging 17-34 nt were gel-excised and ligated with linker oligonucleotides followed by rRNA depletion using Ribo-Zero Gold rRNA

Removal Kit (Illumina). The resultant RNA fragments were reverse transcribed with Photoscript II (NEB) and circularized using CircLigaseII (Epicentre). The circularized cDNA templates were PCR amplified for 6 to 8 cycles using Phusion polymerase (NEB) and sequenced on Illumina Hiseq X (experiment 1) or HiSeq 4000 (experiment 2, 3). For RNA-seq, samples were subjected to library construction using TruSeq Stranded Total RNA Gold (Illumina) and sequenced on HiSeq 4000 as described previously[13]. For analysis, single-end reads (150 bp for experiment 1 and 50 bp for the others) were mapped to mouse genome (GRCm38/mm10) using STAR (version 2.7.0) and were sorted and indexed using samtools (version 1.10). For filtering rRNA and tRNA, STAR was used with rRNA and tRNA annotations downloaded from UCSC table browser. Footprints ranging 20-34 nt were used for further analysis. The periodicity and the A-site location of the reads were determined using fp-framing and fp-transcript (https://github.com/ingolia-lab/RiboSeq), as outlined previously[14].

Generation of Per2::LucTS knockin MEF cells

I used a firefly luciferase containing the mutations T214A, I232A, F295L, and E354K (*LucTS*)[15]. *LucTS* coding sequence was inserted in frame before the endogenous stop codon of *Per2* using CRISPR/Cas9 technology. The gRNA sequence was 5′-TGA GGT ATC ACA GAT TCC CG-3′. The edited genome sequence was verified by PCR-Sanger sequencing. Cells were maintained in Dulbecco's modified Eagle's medium (DMEM)/Ham's F-12 (1:1) supplemented with 10% fetal bovine serum.

Establishment of *Per2* uORF mutant mice and their primary fibroblast cells

Per2 uORF mutant mice (RIKEN BRC No. 11461, https://knowledge.brc.riken.jp/resource/animal/) were established at the Animal Resource Center for Infectious Diseases, Research Institute for Microbial Diseases, Osaka University, by CRISPR/Cas9-based genome editing using C57BL/6J mouse zygotes. The sequences of gRNA and template oligonucleotide were 5′-TTT CCA CTA TGT GAC AGC GGA GG-3′ and 5′-CAA TGG CGC GCG CAG GGG CGG GCT CAG CGC GCG CGG TCA CGT TTT CCA CTT AAC AGC GGA GGG CGA CGC GGC GGC AGC GGC GCT ACT GGG ACT AGC GGC TCC G-3′, respectively. The edited sequence was verified by Sanger DNA sequencing. Primary MLF cells were isolated from the lung of *Per2* uORF mutant mice and control wild-type siblings, as described previously[16]. Cells used for experiments were between passage 2 and 4. The behavioural activities of mice were monitored according to my previously described method[17]. All procedures for animal experiments in this study were conducted in compliance with the Ethical Regulations of Kyoto University and performed under protocols approved by the Animal Care and Experimentation Committee of Kyoto University and the Institutional Animal Care and Use Committees of Osaka university.

Polysome profiling

Linear 15%−50% sucrose gradients were prepared using a BioComp Gradient Master (Biocomp Instruments). Sucrose was dissolved in 20 mM Tris-HCl [pH 7.5], 10 mM $MgCl_2$, 100 mM

KCl, 2 mM DTT, 100 U mL^{-1} human recombinant RNase Inhibitor (TOYOBO), and 100 μg mL^{-1} CHX. Cells were lysed in an ice-cold buffer containing 20 mM Tris-HCl [pH 7.5], 150 mM NaCl, 5 mM $MgCl_2$, 1 mM DTT, 1% Triton X-100, and 100 μg mL^{-1} CHX. Following digestion of genomic DNA with DNase I (~25 U mL^{-1}, Thermo Fisher Scientific), the lysates were centrifuged at 20,000 × *g*. The supernatants were loaded on the top of the gradients and sedimented at 35,000 rpm in a SW41 rotor at 4°C for 2 h. After centrifugation, gradients were fractionated using the Gradient Master instrument with continuous monitoring of A260. RNA in each fraction was extracted using TRIzol LS reagent (Thermo Fisher Scientific).

Immunoblotting

To minimize proteolysis of the endogenous Per2 protein, cells and tissues (dorsal ear skin and lung) were lysed immediately in Laemmli buffer containing 1 × cOmplete Protease Inhibitor cocktail (Roche Diagnostics), as described previously[16, 18]. Immunoblots were performed using my standard method with affinity-purified anti-mPer2 rabbit polyclonal antibody (final concentration, 2 μg ml^{-1})[18] or commercially available antibodies for α-Tubulin (Sigma Aldrich, T6199, 1:1,000), β-actin (Sigma Aldrich, A5441, 1:1000), eIF2α (Cell Signaling, #9722, 1:1000), p-eIF2α (Cell Signaling, #3597, 1:1000), Clock (MBL, D349-3, 1:1,200), Bmal1 (MBL, D335-3, 1:200), Cry2 (MBL, PM082, 1:200), HSF1 (abcam, ab61382, 1:200), p-CREB (Cell Signaling, #9198, 1:1000), and FosB (Cell Signaling, #2251, 1:1000). CHX chase assay was carried out by adding CHX (100 μg ml^{-1}) to the medium at Time 24. Where

specified, cells were treated with 17β-hydroxy Wortmannin (Cayman chemical, 10 μM), PI3-Kinase α Inhibitor 2 (Cayman chemical, 10 μM), GSK1059615 (Cayman chemical, 10 μM), 4EGI-1 (Cayman chemical, 50 μM), GSK2656157 (Cayman chemical, 3 μM), C16 (Sigma Aldrich, 1 μM), A92 (MedChemExpress, 1 μM), ISRIB (Cayman chemical, 1 μM), tunicamycin (Sigma Aldrich, 5 μM), and EGF (Peprotech, 10 ng ml^{-1}).

Metabolic labeling of de novo protein synthesis

Dex-synchronized cells were preincubated with a Met/Cys-free DMEM medium (Thermo Fisher Scientific) for 3 h before experiments. [^{35}S]Methionine (14.8 MBq/sample, Muromachi Kikai) was added to the medium at Time 0 and incubated for 2 h with or without WTS. Cells were lysed in RIPA buffer (50 mM Tris-HCl [pH 8.0], 150 mM NaCl, 0.1% SDS, 1% Nonidet P40, 1% sodium deoxycholate) containing 1 × cOmplete Protease Inhibitor cocktail (Roche Diagnostics) and subjected to immunoprecipitation with anti-mPer2 polyclonal antibody[18] or anti-Cry2 antibody (MBL, PM082). Immunoprecipitants were separated by SDS-PAGE and visualized with X-ray film (Kodak). For click-labeling experiments, azidohomoalanine (AHA) was added, instead of [^{35}S]Methionine, to the medium at Time 0 (final concentration, 50 μM). Cells were lysed in RIPA buffer containing 1 × cOmplete Protease Inhibitor cocktail. Lysates were then conjugated with biotin-PEG4-alkyne (Sigma Aldrich) using Click-iT Protein Reaction Buffer Kit (Thermo Fisher Scientific). After removal of excess free biotin-PEG4-alkyne with PD SpinTrap G-25 columns (Cytiva), AHA-biotin-alkyne labeled proteins

were affinity-purified with streptavidin beads (Thermo Fisher Scientific). The precipitates were analyzed by immunoblotting using anti-mPer2 polyclonal antibody[18], anti-Cry2 antibody (MBL, PM082), or anti-β-actin antibody (Sigma Aldrich, A5441). Biotin-labeled proteins were detected using Vectastain Elite ABC Standard Kit (Vector Laboratories).

LucTS reporter assay

pHSE-LucTS, pCRE-LucTS, and pSRE-LucTS were generated by replacing the Luc coding sequence of pHSE-Luc, pCRE-Luc, and pSRE-Luc (all are from Clontech) with the LucTS. One day after transfection, MEF cells were treated with WTS, heat shock (42°C), 100 μM forskolin, or 50% bovine serum. The mean values of 4-h pre-stimulation baseline of luminescence of pHSE-, pCRE-, and pSRE-LucTS were set to 1. Tet-inducible expression vector pTRE3G (Clontech) was used to construct the *Per2* 5′ UTR-LucTS vectors. The 5′ UTR region of the pTRE3G vector was substituted with the full-length *Per2* 5′ UTR sequence of mouse (NM_011066) or human (XM_006712824) origin. The mutagenesis of the *Per2* uORF was performed using a standard sequential PCR method[16, 17]. For coexpression experiments, the gene encoding eIF2α (*Eif2s1*) was cloned into the *Per2* 5′ UTR-LucTS vectors (at *Eco*RI-*Xho*I site) in conjunction with a Tet-insensitive EF1α promoter. Tet-On 3G NIH3T3 cells were transfected with a plasmid using Viofectin reagent (Viogene). To reduce technical variation between transfections, transfection was performed in a single dish and thereafter the cells were split into test dishes. D-luciferin (Promega) was added to medium before experiments[16].

Cells were treated with doxycycline (1 μg ml^{-1}). Luminescence was continuously monitored using a custom-modified dish-type luminometer AB-2550 Kronos Dio (ATTO), which allows the programming and recording of temperature profiles in real time with an accuracy of 0.1°C. Luminescence was measured for 2 min at 30-min intervals. Values were normalized to the luminescence intensity recorded 30 min before WTS. Fold increase was calculated by dividing the intensity of WTS-treated cells by that of non-treated controls.

Per2::LucTS cell-based kinase inhibitor assay

Per2::LucTS cells were treated with a compound in the Kinase Screening Library (Cayman Chemical, #10505) at a concentration of 10 μM/0.1% DMSO right before WTS application. Score was calculated with the following formula;

$$Score = -log \frac{Td\ of\ tested\ compound}{Td\ of\ vehicle}$$

where *Td* represents the difference in the half-maximum time between WTS and no-WTS cells. The results of compounds which profoundly affect basal LucTS activity were omitted. To see dose dependency, 17β-hydroxy Wortmannin was applied at concentration of 0.3, 1, 10, 30, 100, and 1,000 nM. Where indicated, KNK437 (Sigma Aldrich, 100 μM), Rapamycin (Cayman chemical, 20 nM), MK2206 (Selleck chemicals, 10 μM), U0126 (Cayman chemical, 10 μM), DZnepA (Sigma Aldrich, 100 μM), and Ruthenium Red (Wako, 10 μM) were used.

Quantification of PIP_3 species

Cells were incubated in serum-free medium 1 day before experiments and sampled after 2-h WTS. PIP_3 was measured by an HPLC-MS-based method as described previously[19]. Values were normalized by the sum of the phosphatidylinositol (PI) values.

Quantitative RT-PCR

Total RNA extraction, cDNA synthesis, and quantitative real-time PCR were performed as described previously[16, 17]. *Rplp0* was used as an internal control. The primer sets used in this study were: *Rplp0*, Fw: 5′-CTC ACT GAG ATT CGG GAT ATG-3′, Rv: 5′-CTC CCA CCT TGT CTC CAG TC-3′, and *Per2*, 5′-CTC ACT GAG ATT CGG GAT ATG-3′, Rv: 5′-CTC CCA CCT TGT CTC CAG TC-3′. To quantify *Per2* mRNA levels in the nucleus and cytosol, cellular fractionation was performed as described previously[20].

Statistical analysis

Statistical analyses and plots were performed with GraphPad Prism 8, using statistical test proper for each figure, as indicated. For circular statistics, Rayleigh's uniformity test was performed using Oriana 4 software (Kovacs Computer Services).

Data availability

Ribo-seq and RNA-seq data generated in this study are available from the Gene Expression Omnibus repository under accession number GSE188529.

Results

Chapter 1: Discovery of *Per2* uORF in cells treated with a warm temperature shift

To see a possible effect of a physiological warm temperature shift (WTS, 35°C to 38.5°C) on *Per2* transcription and translation in mammalian cells, I performed RNA-seq and Ribo-seq analyses using dexamethasone-synchronized mouse embryonic fibroblast (MEF) cells with or without WTS treatment at a circadian rising phase of Per2. Cells were grown to full confluence, treated with dexamethasone (Dex) for 3 h to synchronize their endogenous circadian clocks, and subjected to a WTS after 24 h for 2 h, when the endogenous Per2 protein undergoes circadian expression[18] (Fig. 1a). With these conditions, I noticed a quantifiable accumulation of ribosomes at the 5′-flanking region of the main coding sequence of *Per2* mRNA in the WTS-treated cells (Fig. 1b, WTS(+), asterisk). On the other hand, in cells cultured without WTS, these 5′ UTR signals were only scarcely detected (Fig. 1b, WTS(–)). RNA-seq signals were comparable between the WTS-treated and non-treated cells (Fig. 1b, lower tracks). Similar temperature-dependent accumulation of ribosomes at the 5′-flanking region of the main coding sequence of *Per2* was consistently observed in three different sets of experiments (GEO188529). In-depth sequence analysis of each experiment further revealed that this 5′ UTR ribosome accumulation signal on the *Per2* transcript is located on an AUG-UGA minimum ORF sequence, where the initiation codon is immediately followed by a stop

codon, with estimated P-site and A-site located in frame on AUG and UGA, respectively (Fig. 1c, Supplementary Fig 1). This short sequence upstream of the *Per2* CDS, hereafter referred to as *Per2* uORF, is highly conserved among mammalian species including human and mouse (Fig. 1d, Supplementary Fig 1). The identification of a conserved *Per2* uORF whose ribosome coverage changes in response to a mild temperature shift raises the question of whether it relates to physiological temperature entrainment of the clock.

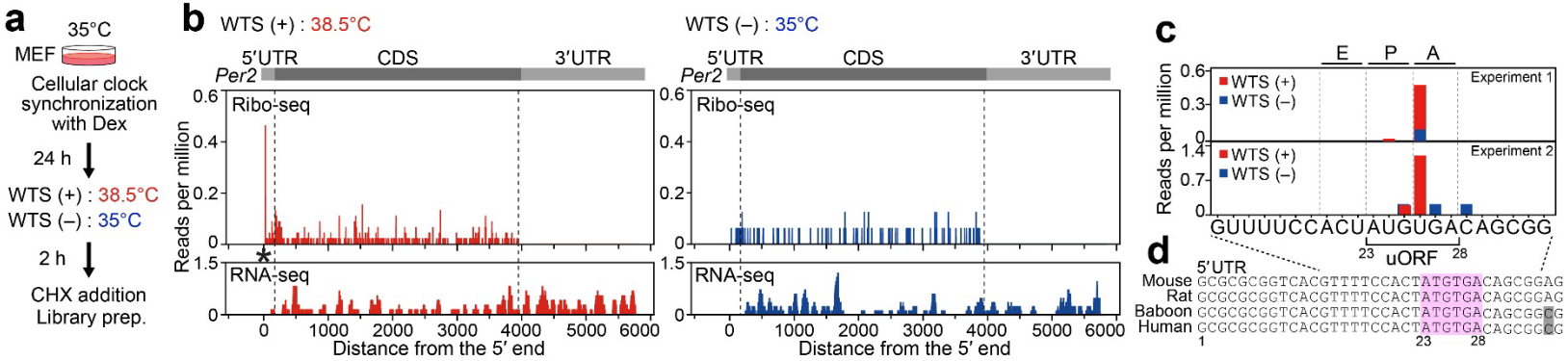
a
35°C
MEF
Cellular clock synchronization with Dex
24 h
WTS (+) : 38.5°C
WTS (–) : 35°C
2 h
CHX addition
Library prep.
b
WTS (+) : 38.5°C
WTS (–) : 35°C
5′UTR
CDS
3′UTR
Per2
Ribo-seq
RNA-seq
Reads per million
Distance from the 5′ end
c
E
P
A
WTS (+)
WTS (–)
Experiment 1
Experiment 2
Reads per million
GUUUUCCACUAUGUGACAGCGG
23
uORF
28
d
5′UTR
Mouse GCGCGCGGTCACGTTTTCCACTATGTGACAGCGGAG
Rat GCGCGCGGTCACGTTTTCCACTATGTGACAGCGGAG
Baboon GCGCGCGGTCACGTTTTCCACTATGTGACAGCGGCG
Human GCGCGCGGTCACGTTTTCCACTATGTGACAGCGGCG

Figure 1 | Identification of a temperature-responsive uORF in the circadian core clock gene *Per2* a, Schematic experimental design for ribosome profiling. MEF cells were incubated with or without a warming temperature shift (WTS, from 35℃ to 38.5℃) for 2 h and processed for Ribo-seq. Dex, dexamethasone. **b,** Distribution of ribosome footprints along the *Per2* gene. Asterisks indicate the position of the uORF in *Per2* 5′ UTR. **c,** Ribo-seq profiles of biological replicate sample, showing WTS-induced accumulation of footprints in the *Per2* uORF. **d,** A conserved uORF sequence in the 5′ UTR region of human, mouse, rat, and baboon *Per2*. Numbers on the alignment indicate the position relative to the mouse *Per2* transcription start site.

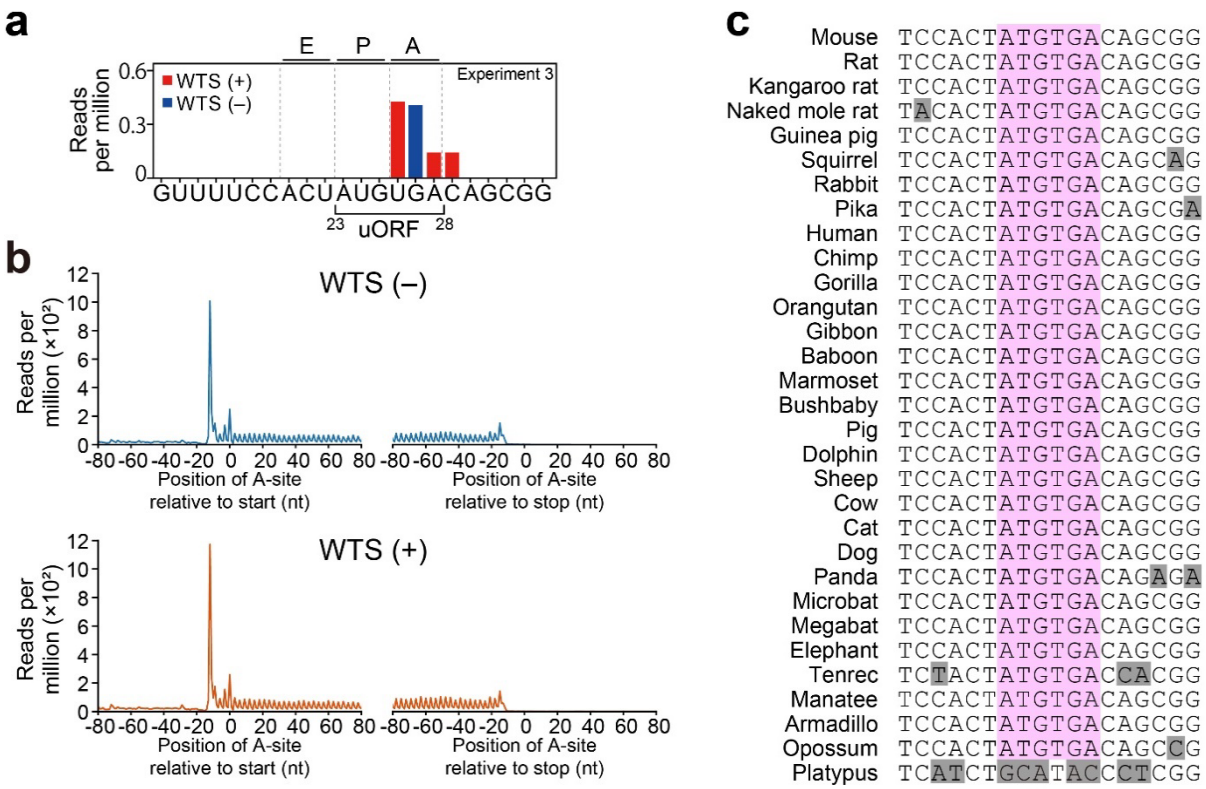

Supplementary Fig. 1 | Identification of *Per2* uORF, related to Fig. 1. a, Ribo-seq profiles of biological replicate samples of Fig. 1b, showing WTS-induced accumulation of footprints in the *Per2* uORF. **b,** Metagene analysis for Ribo-seq read abundance around the start and stop codon from WTS-treated or non-treated cells. The abundance of 29-nt reads with 5′ ends at each indicated position is shown. In both samples, the reads are restricted to coding sequences and exhibit 3-nucleotide periodicity. Read counts were normalized by sequencing depth. The sum from three replicates is shown. **c,** *Per2* uORF sequences in mammalian species. Non-conserved nucleotides are shown in gray shadow and the conserved uORF is highlighted in pink.

Chapter 2: Temperature-dependent control of Per2 protein synthesis depends on uORF.

A physiological temperature might modulate the oscillating levels of the endogenous Per2 protein. To test this, I performed protein blot analysis using cells treated with WTS at 0, 4, 8, 12, 16, 20, 24 and 28 h after synchronization (Fig. 2a) and found the capability of WTS to increase Per2 protein expression in a manner depending on the time of WTS applied. When applied at Time 0, 4, 20, 24, and 28, which correspond to Per2 protein rising phase, WTS led to a greater Per2 expression (Fig. 2a, see arrowheads: at each time-point, increase was more profound in a lower band). WTS had little effect on the expression profiles of Per2 in its decreasing phase, Time 8, 12, or 16. Application of WTS did not influence the expression of α-tubulin or other clock core proteins (Extended Data Fig. 1a). Immunoblots of Per2 protein from the mouse lung and ear skin cultures in the presence or absence of WTS also reproduced the temperature-responsive increment of the endogenous Per2 protein expression (Extended Data Fig. 1b).

Despite the change in the Per2 protein expression by WTS, the *Per2* transcript levels were nearly unaffected by the same treatment at any timepoints tested (Fig. 2a). This was further supported by a little or marginal effect of WTS on transcription through the heat-shock element (HSE), cAMP/Ca^{2+} response element (CRE), and serum response element (SRE), all known to have the ability to affect *Per2* transcription through its promoter[21-23] (Extended Data Fig.

1c,d). WTS has little effect on the intracellular localization of *Per2* transcript (Extended Data Fig. 1e). The Per2 protein stability, assessed by cycloheximide (CHX) treatment, also remained virtually unchanged by WTS (Extended Data Fig. 1f). Consistently, [^{35}S]methionine- or click-labeling experiments and polysome profiles obtained by sucrose gradient sedimentation (Fig. 2b,c, Extended Data Fig. 1g) verified an increase in protein synthesis of Per2 after WTS treatment.

Primary mouse lung fibroblast (MLF) cells were next prepared from wild-type (wt) mice and newly generated *Per2* uORF mutant (mut) mice (Supplementary Fig. 2), in which the original *Per2* ATG-TGA sequence was mutated to TAA. Notably, in contrast to the control wt cells, WTS was unable to affect Per2 expression in *Per2* uORF mut cells ($P = 0.3864$, WTS(–) versus (+) in mut cells; $P = 0.0005$, for wt cells, Fig. 2d). In both basal and WTS-treated cells, *Per2* transcript levels were comparable between wt and uORF mut cells (Fig. 2d), excluding the possibility that *Per2* transcription was affected by the mutation. Intact full-length *Per2* genome sequence except for the mutation and normal circadian locomotor activity rhythm displayed by the mutant mice (Supplementary Fig. 2) suggested that the removal of the *Per2* uORF is not deleterious for the rhythm generation. Rather, this UTR sequence appears to have a more limited role in modulating the temperature response of Per2 expression.

The function of the *Per2* UTR sequence was examined further using reconstituted luciferase

reporters. The region of the human and mouse *Per2* 5′ UTR containing the minimum uORF sequence, cloned into a reporter vector adopting the thermostable version firefly luciferase[15], conferred WTS response to the reporter (Fig. 2e, ~70% increase compared with no *Per2* 5′ UTR vector), which disappeared in the constructs in which the uORF was mutated from ATGTGA to TAA. Disruption of the minimal uORF sequence by means of ATG mutation, stop codon mutation, or extra codon insertion between ATG and TGA also nullified the responsiveness to WTS (Fig. 2f). Disruption of the Kozak sequence upstream of the uORF also abrogated the WTS responsiveness (Fig. 2f; see also Extended Data Fig. 1h). These data indicate that the isolated *Per2* 5′ UTR containing the uORF suffices to impart temperature dependence to the downstream reporter translation.

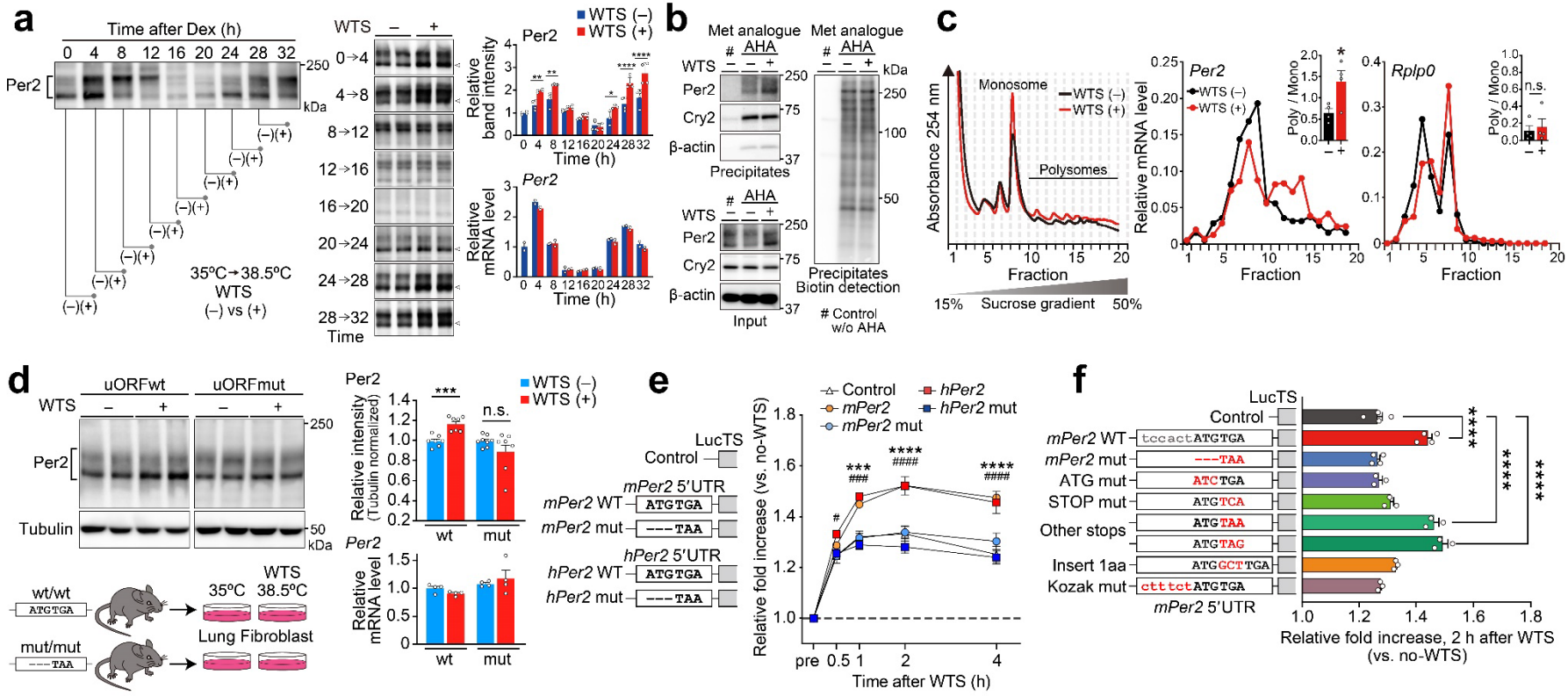
a
Time after Dex (h)
0 4 8 12 16 20 24 28 32
Per2
250
kDa
(–)(+)
35°C→38.5°C
WTS
(–) vs (+)
WTS – +
0→4
4→8
8→12
12→16
16→20
20→24
24→28
28→32
Time
WTS (–)
WTS (+)
Per2
Relative band intensity
Time (h)
Relative mRNA level
b
Met analogue
AHA
WTS
Per2
Cry2
β-actin
Precipitates
Input
Precipitates
Biotin detection
Control w/o AHA
c
Monosome
Polysomes
Absorbance 254 nm
Fraction
15%
Sucrose gradient
50%
Relative mRNA level
Per2
Rplp0
Poly / Mono
n.s.
d
uORFwt
uORFmut
Tubulin
wt/wt
mut/mut
ATGTGA
---TAA
35°C
38.5°C
Lung Fibroblast
Relative intensity (Tubulin normalized)
n.s.
wt
mut
e
LucTS
Control
mPer2 5′UTR
mPer2 WT
mPer2 mut
hPer2 5′UTR
hPer2 WT
hPer2 mut
Control
mPer2
mPer2 mut
hPer2
hPer2 mut
Relative fold increase (vs. no-WTS)
Time after WTS (h)
pre 0.5 1 2 4
f
LucTS
Control
mPer2 WT
mPer2 mut
ATG mut
STOP mut
Other stops
Insert 1aa
Kozak mut
mPer2 5′UTR
tccactATGTGA
---TAA
ATCTGA
ATGTCA
ATGTAA
ATGTAG
ATGGCTTGA
ctttctATGTGA
Relative fold increase, 2 h after WTS (vs. no-WTS)

Figure 2 | *Per2* minimal uORF mediates temperature-dependent Per2 protein translation. **a,** Per2 protein accumulation in the presence or absence of WTS at different circadian time points. Sampling was performed using Dex-synchronized MEF cells. Per2 protein and mRNA quantification data are shown in the right graphs. Relative mRNA levels were measured by qRT-PCR. Error bars indicate variation of two independent experiments. Protein blot data were analyzed by densitometry ($n = 4$ for each condition). $^{**}P = 0.0020$, Time 4; $^{**}P = 0.0015$, Time 8; $^{*}P = 0.0478$, Time 24; $^{****}P < 0.0001$, Times 28 and 32. **b,** Immunoblots of newly synthesized Per2 protein. After being placed into Met-free culture medium, cells were exposed to WTS in the presence of azidohomoalanine (AHA). The lysates were subjected to click chemistry. Biotin-labeled proteins were purified and probed for either Per2 or biotin. **c,** Representative polysome profiles obtained by sucrose gradient sedimentation of cytoplasmic extracts from WTS-treated or non-treated MEF cells. The right two panels show qRT-PCR-determined mRNA levels of *Per2* or *Rplp0*. Insets show polysome to monosome ratio of each transcript ($n = 4$ independent experiments). $^{*}P = 0.0391$. **d,** Immunoblots showing WTS-dependent accumulation of Per2 protein in WT and *Per2* uORF mutant MLF cells. Bar graphs show relative abundance of Per2 protein or mRNA: Protein levels were determined by densitometry ($n = 4$ per condition). $^{***}P = 0.0005$. **e,** Luciferase reporter activity traces of *Per2* uORF-dependent translation after WTS ($n = 4$). Reporter constructs containing either human or mouse *Per2* 5′ UTR, or their mutants devoid of the uORF were transiently introduced into NIH3T3 Tet-On 3G cells. Cells were treated with doxycycline, and WTS was applied after 3 h. $^{***}P = 0.0001$, $^{****}P < 0.0001$ (control vs *mPer2* WT); $^{\#}P = 0.0203$, $^{\#\#\#\#}P < 0.0001$ (control vs *hPer2* WT). TS, thermostable. **f,** Fold increase of WT and different mutant series of the *Per2* uORF. The structure of the *Per2* minimal uORF was disrupted by mutation, deletion, or insertion. Reporter assays were performed as described in **e**. $n = 3$ independent experiments except $n = 4$ for control, *mPer2* WT, *mPer2* mut. $^{****}P < 0.0001$. Values show mean ± s.e.m., otherwise indicated. Statistics in c, d were unpaired two-sided Student's *t*-test; statistics in a, e were Two-way ANOVA followed by Holm-Sidak *post hoc* tests; statistics in f were One-way ANOVA followed by Dunnett's multiple comparisons test.

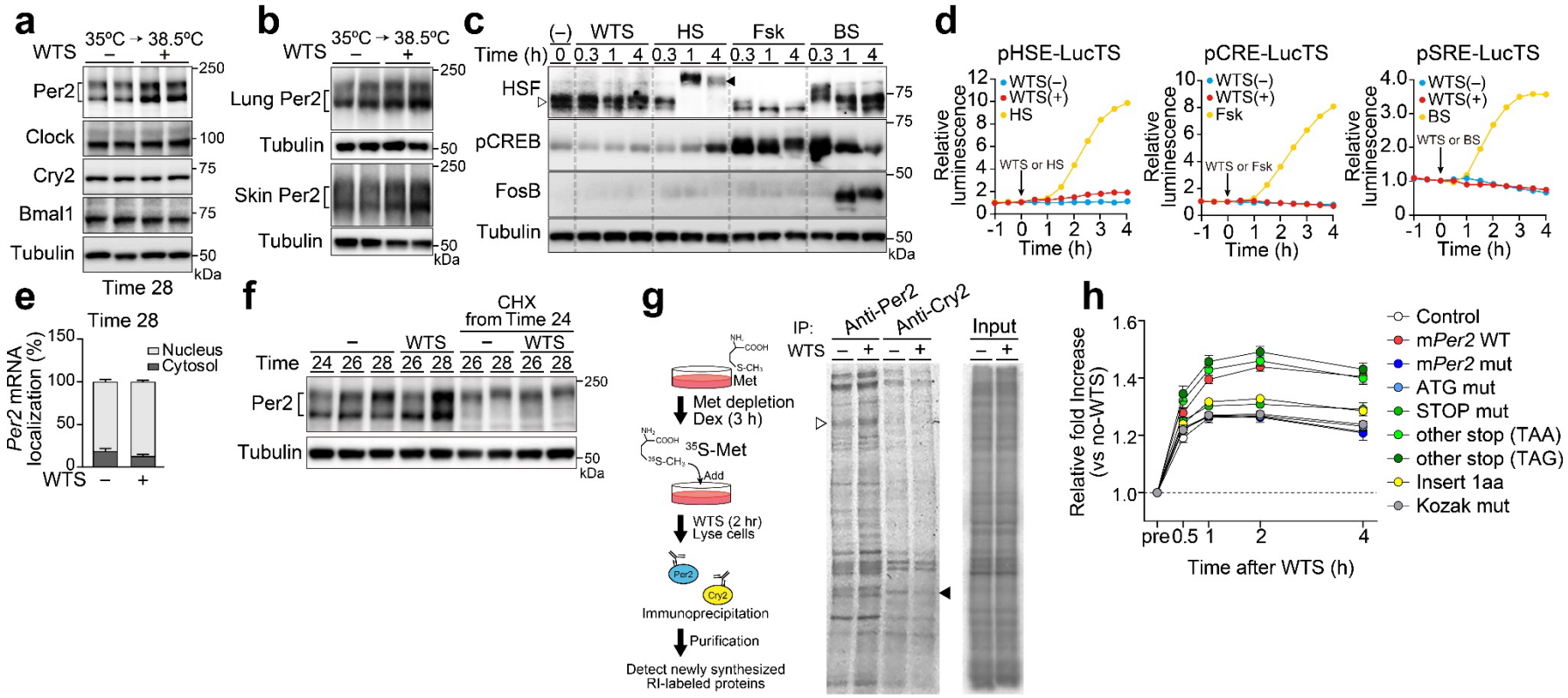
a
WTS 35ºC → 38.5ºC
Per2
Clock
Cry2
Bmal1
Tubulin
Time 28
b
Lung Per2
Skin Per2
c
Time (h)
HSF
pCREB
FosB
d
pHSE-LucTS
pCRE-LucTS
pSRE-LucTS
Relative luminescence
Time (h)
e
Per2 mRNA localization (%)
Nucleus
Cytosol
f
CHX from Time 24
Time
g
IP:
Anti-Per2
Anti-Cry2
Input
Met depletion
Dex (3 h)
35S-Met
WTS (2 hr)
Lyse cells
Immunoprecipitation
Purification
Detect newly synthesized RI-labeled proteins
h
Relative fold Increase (vs no-WTS)
Time after WTS (h)
Control
mPer2 WT
mPer2 mut
ATG mut
STOP mut
other stop (TAA)
other stop (TAG)
Insert 1aa
Kozak mut

Extended Data Fig. 1 | WTS-dependent Per2 protein accumulation involves regulation at the translation level, related to Fig. 2. a, Immunoblots of Per2, Clock, Cry2, and Bmal1 in MEF cells with or without WTS. **b,** Immunoblots of Per2 protein from the mouse lung and ear skin cultures in the presence or absence of WTS. The tissues were isolated at ZT12 and cultured in dish at 35°C or 38.5°C for 2 h. **c,** Immunoblots showing an absence of increase in HSF phosphorylation, CREB phosphorylation, and FosB expression after WTS. Heat shock (HS, 42°C), forskorin (Fsk), and bovine serum (BS) served as positive control for HSF, pCREB, and FosB induction, respectively. A closed arrowhead on the blot shows the position of phosphorylated HSF. Unphosphorylated HSF is indicated by the open arrowhead. **d,** A little or minor effect of WTS on transcription from the heat-shock element (HSE), cAMP/Ca^{2+} response element (CRE), or serum response element (SRE). LucTS reporters containing HSE, CRE, or SRE were transiently introduced into MEF cells. **e,** Quantification of *Per2* mRNA in nuclear and cytoplasmic fractions of WTS-treated or non-treated cells. Bar height represents the contribution of each fraction to total cellular mRNA (100%). **f,** Unaffected Per2 protein stability in WTS-treated cells determined by cycloheximide (CHX) chase assay. WTS and/or CHX was applied at Time 24 (Per2 protein rising phase). **g,** Newly synthesized Per2 protein determined by immunoprecipitation of [^{35}S]methionine-labelled cell lysates. Immuno-precipitation was performed with antibodies against Per2 or Cry2. Arrowheads indicate the position of either Per2 or Cry2. **h,** The fold increases in reporter activity of *Per2* LucTS constructs from their pre-WTS basal values, related to Fig. 2f. The reporter constructs shown in Fig. 2f were examined. Their response to WTS was assessed as described in Fig. 2e. The values are the mean ± s.e.m. $n = 3$ independent experiment except $n = 4$ for control, *mPer2* WT, *mPer2* mut.

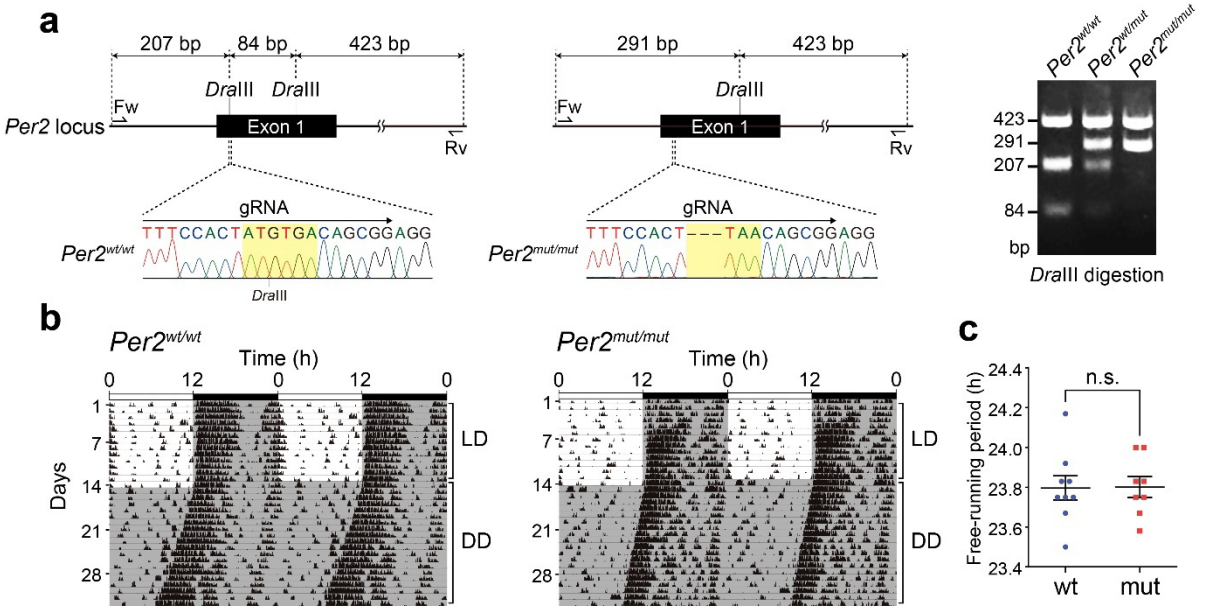

Supplementary Fig. 2 | Generation of mice carrying a targeted mutation at the *Per2* uORF, related to Fig. 2d. a, Genome modification strategy using the CRISPR/Cas9 system. The ATG-TGA *Per2* uORF was mutated to TAA. DNA sequencing chromatograms of wild-type (wt/wt) and mutant (mut/mut) mice confirmed the sequence of unmodified and modified uORF. The mutation causes the loss of *Dra*III site, which was utilized for PCR genotyping. **b,** Representative locomotor activity records of *Per2*$^{wt/wt}$ and *Per2*$^{mut/mut}$ mice. Mice were housed in a 12-h light:12-h dark cycle (LD) for 2 weeks and released into constant darkness (DD). Locomotor activity was detected with passive infrared sensors. Periods of darkness are indicated by grey backgrounds. Data are shown in double-plotted format. Each horizontal line represents 48 h; the second 24-h period is plotted to the right and below the first. **c,** Circadian free-running period of locomotor activity rhythm in DD. Period was determined with χ^2 periodogram, based on animal behaviours in a 21-day interval taken 3 days after the start of DD. Plots are periods of individual mice. wt, n = 9; mut, n = 8 for mut. Bars indicate mean ± s.e.m. n.s., not significant.

Chapter 3: Blocking phosphoinositide 3-kinase abrogates WTS response of Per2 expression.

I next pharmacologically examined potential mediators of the Per2 WTS response. Blocking the pathway mediated by the eukaryotic translation initiation factor eIF4Eusing its inhibitor 4EGI-1 had little effect on the WTS-induced Per2 protein expression, making it unlikely that cap-dependent mRNA regulation is involved in the thermal Per2 regulation unlikely (Extended Data Fig. 2a). In contrast, inhibiting the integrated stress response related kinases PERK and PKR, but not GCN2, led to a reduction in WTS response of Per2 expression (Extended Data Fig. 2b). WTS brings about an increased phosphorylation of the eukaryotic translation initiation factor eIF2α in a PERK/PKR-dependent manner (Extended Data Fig. 2c); however, eIF2α itself was not essential for the thermal Per2 expression, as blocking the pathway mediated by phosphorylated eIF2α using its inhibitor ISRIB failed to abrogate the Per2 response (Extended Data Fig. 2d), and as expression of neither constitutively active eIF2α (eIF2α-S51D) nor its dominant negative form (eIF2α-S51A) compromised the WTS response of the *Per2* uORF-dependent translation (Extended Data Fig. 2e).

As a tool to identify yet unknown additional mediators contributing to the WTS response of Per2 expression, I generated Per2::LucTS knock-in MEF cells, in which the thermostable luciferase[15] (LucTS) was fused to the endogenous Per2 (Fig. 3a; see Extended Data Fig. 2f for

thermostability of LucTS compared to wt Luc). This knock-in reporter activity recapitulated the Per2 expression in terms of its circadian-rising-phase-specific reaction (Fig. 3a) and the sensitivity to WTS, which changes as a function of temperature applied (Extended Data Fig. 2g). Screening of 155 kinase inhibitors and follow-up validation by western blot analysis led to the identification of 4 chemicals that could abrogate the response of the endogenous Per2 protein expression to WTS (Fig. 3b,c, Extended Data Fig. 2h,i). Notably, all 4 inhibitors share common targets: the phosphoinositide 3-kinases, PI3Ks, which have been implicated in cellular heat stress signaling[24-26]. Extending its potential contribution to innocuous WTS response, LC-MS/MS analysis revealed that phosphatidylinositol 3,4,5-trisphosphate, PIP_3, which is the the primary product of PI3K reaction, was increased by the temperature shift from 35°C to 38.5°C (Supplementary Fig. 3, Fig. 3d). The specific PI3K inhibitor 17β-hydroxy wortmannin (hereafter abbreviated Wortm) blocked this upregulation of PIP_3. Moreover, Wortm blocked WTS response of Per2 in a dose-dependent manner with IC_{50} of 20 nM, similar to previous studies[27, 28] (Extended Data Fig. 2j, Supplementary Fig. 3).

To test further my PI3K-Per2 axis model, I sought to activate PI3K by alternative stimulus. For this purpose, I used epidermal growth factor (EGF), which is known to activate the PI3K pathway[29] and has been shown to enhance expression of *Per2* at both the transcription and the protein-translation levels through an yet-unidentified mTOR-independent pathway[30]. EGF treatment resulted in augmented Per2 protein expression, which was blocked by Wortm (Fig.

3e). Furthermore, the endogenous uORF in *Per2* was necessary for the enhancement of Per2 protein expression after EGF treatment (Fig. 3f). I verified that *Per2* transcript levels were almost equivalent between wt and mut cells before and after the EGF treatment (Fig. 3e,f).

I examined inhibitors toward mTOR (rapamycin), Akt (MK2206), MEK (U0126), heat shock factor 1 (KNK437), TRP channel (Ru red), and m6A methylation[20, 31] (DZnep), but none of them displayed inhibitory effect on WTS response of Per2::LucTS (Extended Data Fig. 2k). PI3K inhibition thus appears to be unique in strongly diminishing the Per2 WTS response.

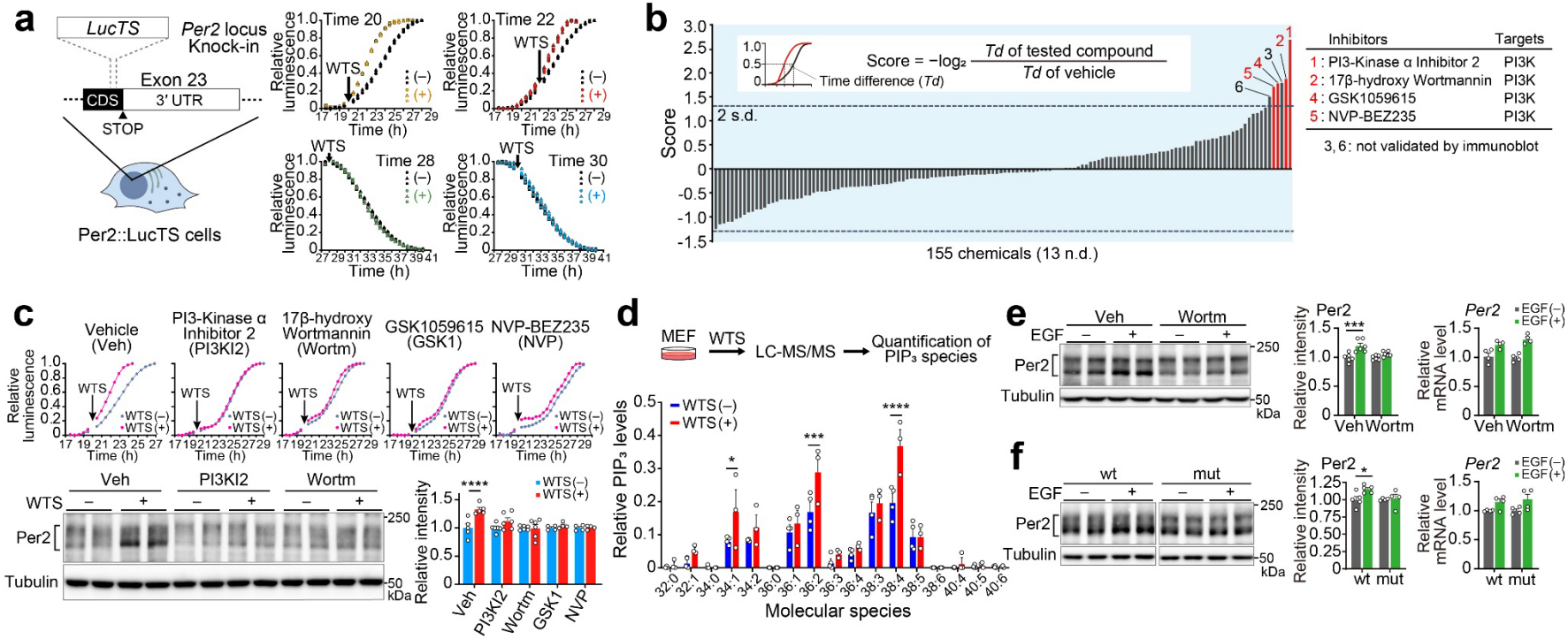
a
LucTS
Per2 locus Knock-in
Exon 23
CDS
3′ UTR
STOP
Per2::LucTS cells
Relative luminescence
Time 20
Time 22
Time 28
Time 30
WTS
(–)
(+)
Time (h)
b
Score = −log₂ Td of tested compound / Td of vehicle
Time difference (Td)
Score
2 s.d.
155 chemicals (13 n.d.)
Inhibitors
Targets
1 : PI3-Kinase α Inhibitor 2 PI3K
2 : 17β-hydroxy Wortmannin PI3K
4 : GSK1059615 PI3K
5 : NVP-BEZ235 PI3K
3, 6 : not validated by immunoblot
c
Vehicle (Veh)
PI3-Kinase α Inhibitor 2 (PI3KI2)
17β-hydroxy Wortmannin (Wortm)
GSK1059615 (GSK1)
NVP-BEZ235 (NVP)
WTS(–)
WTS(+)
Veh
PI3KI2
Wortm
Per2
Tubulin
kDa
Relative intensity
d
MEF
WTS
LC-MS/MS
Quantification of PIP₃ species
Relative PIP₃ levels
Molecular species
e
Veh
Wortm
EGF
Per2
Tubulin
Relative intensity
Relative mRNA level
EGF(–)
EGF(+)
f
wt
mut

Figure 3 | PI3K mediates temperature response of Per2 translation. a, Reporter activity traces of Per2::LucTS knock-in cells in the presence or absence of WTS at a rising phase (Time 20, 22) or decreasing phase (Time 28, 30) of Per2 expression. Plots indicate three biological replicates. LucTS encodes a thermostable luciferase. **b,** Kinase inhibitor screening leading to the identification of PI3K as a potential mediator of WTS-dependent Per2 translation. The horizontal dashed line indicates the threshold of 2 s.d. Red, PI3K inhibitors. **c,** Per2::LucTS traces showing the effect of PI3K inhibitors on WTS-dependent Per2 translation. WTS was applied in Per2 protein rising phase (20 h after Dex synchronization) in the presence or absence of indicated PI3K inhibitors. Western blots show the expression of the endogenous Per2 in MEF cells treated with the same inhibitors. Protein blot data were analyzed by densitometry. Veh, $n = 5$; PI3KI2, Wortm, $n = 6$; GSK1, NVP, $n = 4$. ****$P < 0.0001$. **d,** Mass spectrometry profiling of PIP_3 species in cultured MEF cells with or without WTS. Values were normalized by total PIP_3 levels of no-WTS group. WTS(–), $n = 4$, WTS(+), $n = 3$. *$P = 0.0347$, ***$P = 0.0010$, ****$P < 0.0001$. **e,** EGF-induced increase of Per2 protein accumulation and its inhibition by 17β-hydroxy wortmannin. Cells were treated with EGF for 2 h. Per2 protein and mRNA quantification data are shown in the right graphs. Relative mRNA levels were measured by qRT-PCR ($n = 4$). Protein blot data were analyzed by densitometry ($n = 6$). ***$P = 0.0002$. **f,** Immunoblots examining EGF-dependent Per2 protein accumulation in WT or *Per2* uORF mutant MLF cells. Per2 protein and mRNA quantification data are shown in the right graphs. Relative mRNA levels were measured by qRT-PCR ($n = 4$). Protein blot data were analyzed by densitometry. wt, $n = 5$; mut, $n = 4$. *$P = 0.0245$. Two-way ANOVA followed by Sidak's multiple comparisons test. Error bars indicate s.e.m.

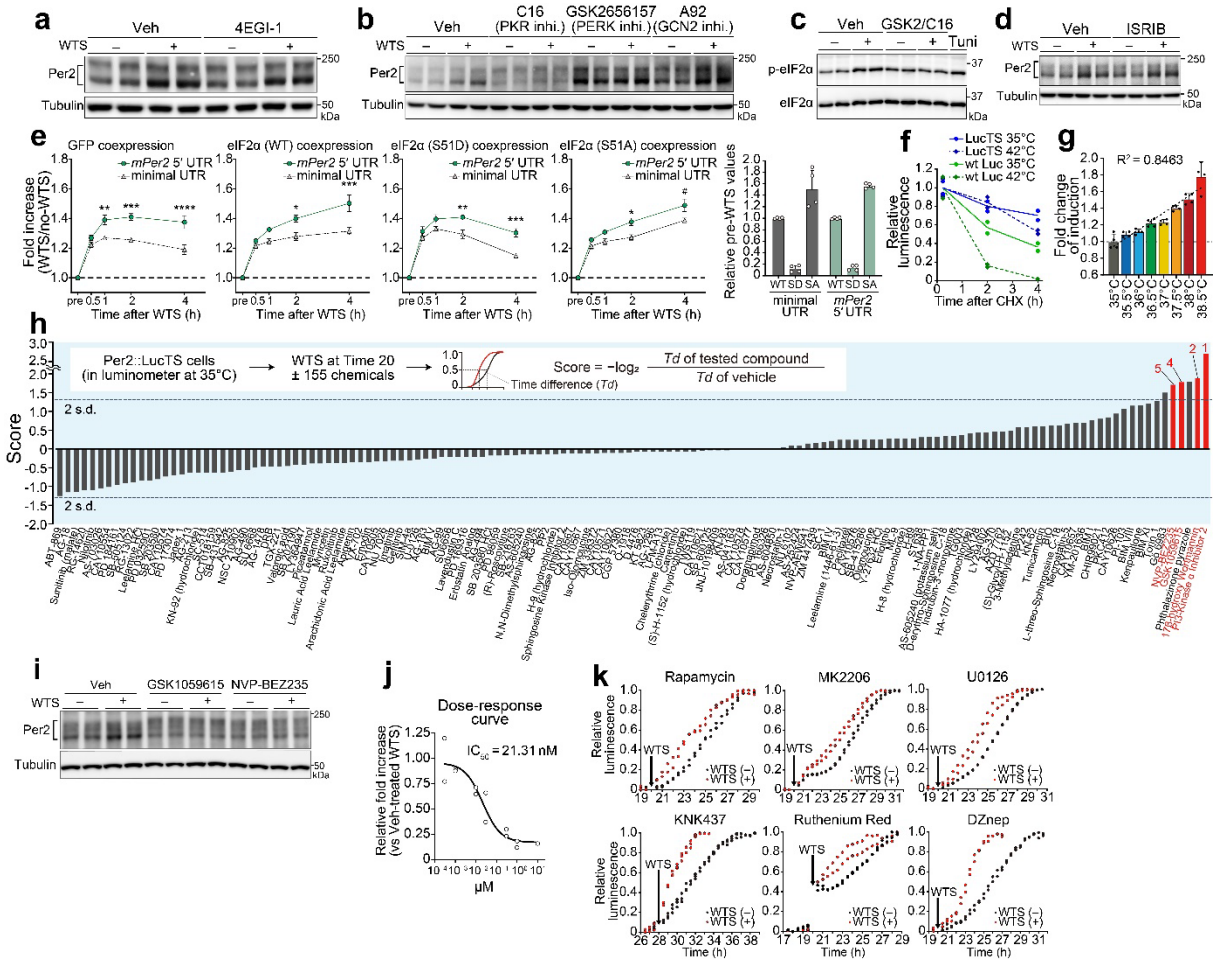
a
Veh
4EGI-1
WTS
Per2
Tubulin
250
50
kDa
b
Veh
C16 (PKR inhi.)
GSK2656157 (PERK inhi.)
A92 (GCN2 inhi.)
c
Veh
GSK2/C16
Tuni
p-eIF2α
eIF2α
37
d
Veh
ISRIB
e
GFP coexpression
eIF2α (WT) coexpression
eIF2α (S51D) coexpression
eIF2α (S51A) coexpression
mPer2 5′ UTR
minimal UTR
Fold increase (WTS/no-WTS)
Time after WTS (h)
Relative pre-WTS values
WT SD SA
minimal UTR
mPer2 5′ UTR
f
LucTS 35°C
LucTS 42°C
wt Luc 35°C
wt Luc 42°C
Relative luminescence
Time after CHX (h)
g
R² = 0.8463
Fold change of induction
35°C
35.5°C
36°C
36.5°C
37°C
37.5°C
38°C
38.5°C
h
Per2::LucTS cells (in luminometer at 35°C)
WTS at Time 20 ± 155 chemicals
Score = −log₂ Td of tested compound / Td of vehicle
Time difference (Td)
Score
2 s.d.
i
Veh
GSK1059615
NVP-BEZ235
j
Dose-response curve
IC50 = 21.31 nM
Relative fold increase (vs Veh-treated WTS)
μM
k
Rapamycin
MK2206
U0126
KNK437
Ruthenium Red
DZnep
Relative luminescence
WTS
WTS (–)
WTS (+)
Time (h)

Extended Data Fig. 2 | Pharmacological characterization of Per2 response to WTS, related to Fig. 3. a, Immunoblots of the Per2 levels with or without WTS in the presence or absence of 4EGI-1. 4EGI-1 is an inhibitor of cap-dependent translation. **b,** Immunoblots examining the effects of different eIF2α kinase inhibitors on WTS-dependent Per2 expression. C16, GSK2656157, and A92 are inhibitors for PKR, PERK, and GCN2, respectively. **c,** Immunoblots showing increased phosphorylation of eIF2α in WTS-treated cells. GSK2656157 and C16 were used in conjunction. Tunicamycin (Tuni) was used to induce eIF2α phosphorylation. **d,** Immunoblots showing unaffected WTS-induced Per2 expression in the cells treated with the inhibitor of p-eIF2α-mediated signaling, ISRIB. **e,** Luciferase activity traces of *Per2* uORF-dependent translation in cells expressing eIF2α, its constitutively active form (eIF2α S51D), or dominant negative form (eIF2α S51A). GFP serves as control. Right bar graph shows pre-WTS basal values of each condition. Indicating the effectiveness of expressed eIF2α-mutants, the basal values were either decreased or increased by S51D or S51A, respectively. Note that even under these conditions WTS-induced *Per2* 5′ UTR response was unaffected. $n = 3$ for each experiment. GFP, $^{**}P = 0.0079$, $^{***}P = 0.0007$, $^{****}P < 0.0001$; eIF2α, $^{*}P = 0.0117$, $^{***}P = 0.0001$; eIF2α S51D, $^{**}P = 0.0041$, $^{***}P = 0.0002$; eIF2α S51A, $^{*}P = 0.0112$, $\#P = 0.0141$, minimal UTR vs mPer2 5′ UTR. **f,** Comparisons of luciferase activity stability of LucTS and Luc (original firefly Luc) in MEF cells cultured at 35°C or 42°C. CHX was applied at Time 0. **g,** Fold increase of reporter activity of Per2::LucTS MEF cells under different degrees of temperature shift. Temperature was increased from 35°C to the indicated degrees for 2 h. **h,** Inhibitors used for the kinase screening in Fig. 3a. Scoring was performed based on the difference in the half-maximum time between WTS and no-WTS cells. The horizontal dashed lines indicate the 2 s.d. of 142 compounds that were able to be reliably scored. **i,** Immunoblots showing the expression of the endogenous Per2 with or without WTS in the presence or absence of GSK1059615 or NVP-BEZ235. **j,** A dose-dependent inhibitory effect of 17β-hydroxy wortmannin on WTS-dependent Per2::LucTS reporter activity. Reporter activity traces of Per2::LucTS cells with or without WTS in the presence of Rapamycin, the mTOR inhibitor, MK2206, the Akt inhibitor, U0126, the MEK inhibitor, KNK437, the heat shock signaling inhibitor, Ruthenium red, the TRPV inhibitor, and DZnep, the global methylation inhibitor.

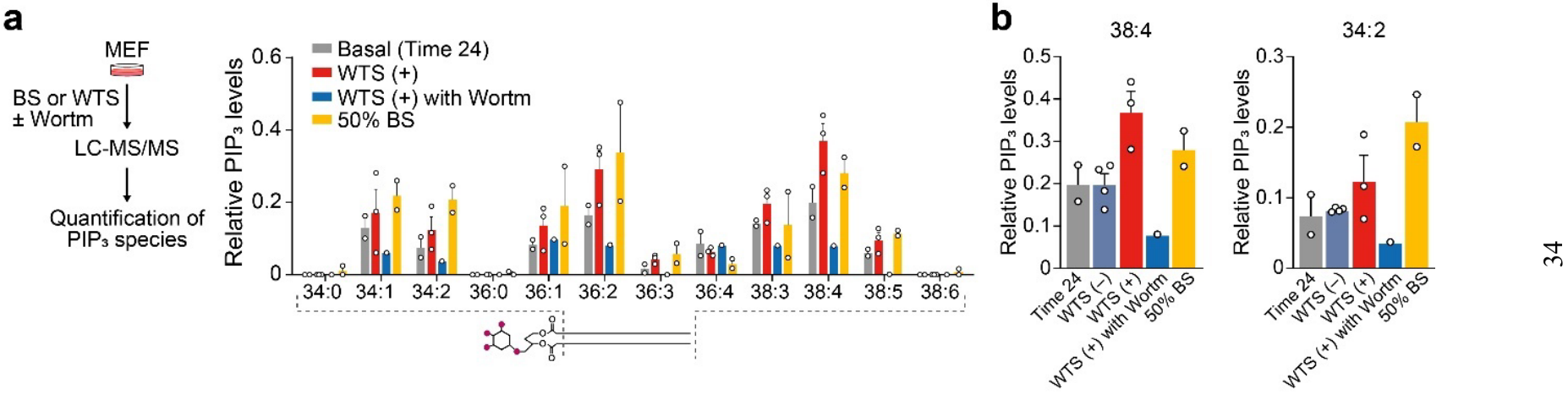
a
MEF
BS or WTS
± Wortm
LC-MS/MS
Quantification of
PIP₃ species
Relative PIP₃ levels
0.6
0.4
0.2
0
Basal (Time 24)
WTS (+)
WTS (+) with Wortm
50% BS
34:0
34:1
34:2
36:0
36:1
36:2
36:3
36:4
38:3
38:4
38:5
38:6
b
38:4
34:2
Relative PIP₃ levels
0.5
0.4
0.3
0.2
0.1
0
Time 24
WTS (–)
WTS (+)
WTS (+) with Wortm
50% BS

Supplementary Fig. 3 | Comparisons of PIP3 profiles between WTS-treated and BS-treated cells, related to Fig. 3c. a, Mass spectrometry profiling of PIP_3 species in WTS-treated and BS-treated cells. WTS was provided alone or in combination with the PI3K inhibitor 17β-hydroxy wortmannin (Wortm). **b**, Different profiles of response of C38:4 PIP_3 (left) and C34:2 PIP_3 (right) to WTS and BS treatment. Values were normalized by the levels of total PIP3s of no-WTS group. The data of WTS (+) and (–) were reproduced from Fig. 3c.

Chapter 4: *Per2* uORF and PI3K mediate circadian clock temperature entrainment.

Because the temperature cycle within the body is not square-wave, I tested the response of cells to thermal cycles that resemble body temperature (Fig. 4). Using telemetry, I measured abdominal body temperature of mice and calculated a mean 24-h body temperature profile[32] (Fig. 4a–c). Cells were first synchronized by Dex treatment and released into either constant (35°C) or simulated body temperature conditions over 92 h. As reported previously[8], in wt cells, the simulated body temperature was capable of enhancing the rhythm amplitude of Per2 protein expression lasting over 4 circadian cycles (Fig. 4a; see also Supplementary Fig. 5). In contrast, the simulated body temperature cycle was not able to efficiently enhance the rhythm sustainability of Per2 protein expression in *Per2* uORF mut cells (Fig. 4a), with its 1st-cycle-versus-3rd-cycle damping rate being significantly lower than that of wt cells (Fig. 4a, inset). The initiation of Per2 protein expression after Dex treatment was almost similar between wt and mut cells. Moreover, in constant temperature conditions, the damping rates of the two genotypes were not significantly different (Fig. 4a, Supplementary Fig. 5), suggesting that Per2 protein expression in the mut cells appeared normal except for temperature dependency.

Examining the effect of Wortm on Per2::LucTS rhythm further revealed an attenuating effect of Wortm treatment on the maintenance of amplitude of Per2::LucTS rhythm under simulated body temperature conditions (Veh vs. Wortm, $P = 0.0045$, on day 7, $P = 0.0078$, on day 8, Fig.

4b). A reduced, but remaining rhythm was, however, found in Wortm-treated cells, implying a participation of other regulatory factor(s) in the enhancement of the Per2 rhythm amplitude.

I finally examined the ability of thermal cycles to entrain the phase of oscillatory Per2 expression rather than merely amplifying its circadian amplitude. I prepared Per2::LucTS cell cultures with different phases, each separately synchronized by Dex treatment 6-h apart (Fig. 4c) and subjected to simulated body temperature cycles with a shared synchronous phase. After several days in culture, the Per2::LucTS rhythmic expression adapted to the shared simulated body temperature cycles. In Fig. 4c, to emphasize the phase of the rhythms, the values were normalized using 24-h standard deviation of luminescence. By days 7–8, the phases of all tested cultures converged to a common phase (Fig. 4c, upper), resulting in a significant increase in phase uniformity value (Rayleigh's uniformity test, $P < 0.0001$). In contrast, when the cells were cultured in the presence of Wortm, the temperature cycles no longer robustly synchronized the phase of Per2::LucTS rhythms (Fig. 4c, lower), with the resultant phases on days 7–8 remaining diverge (Rayleigh's uniformity test, $P = 0.999$). These results demonstrate that the PI3K-mediated signaling is indispensable for the proper phase entrainment by the simulated physiological body temperature cycles (Fig. 4d).

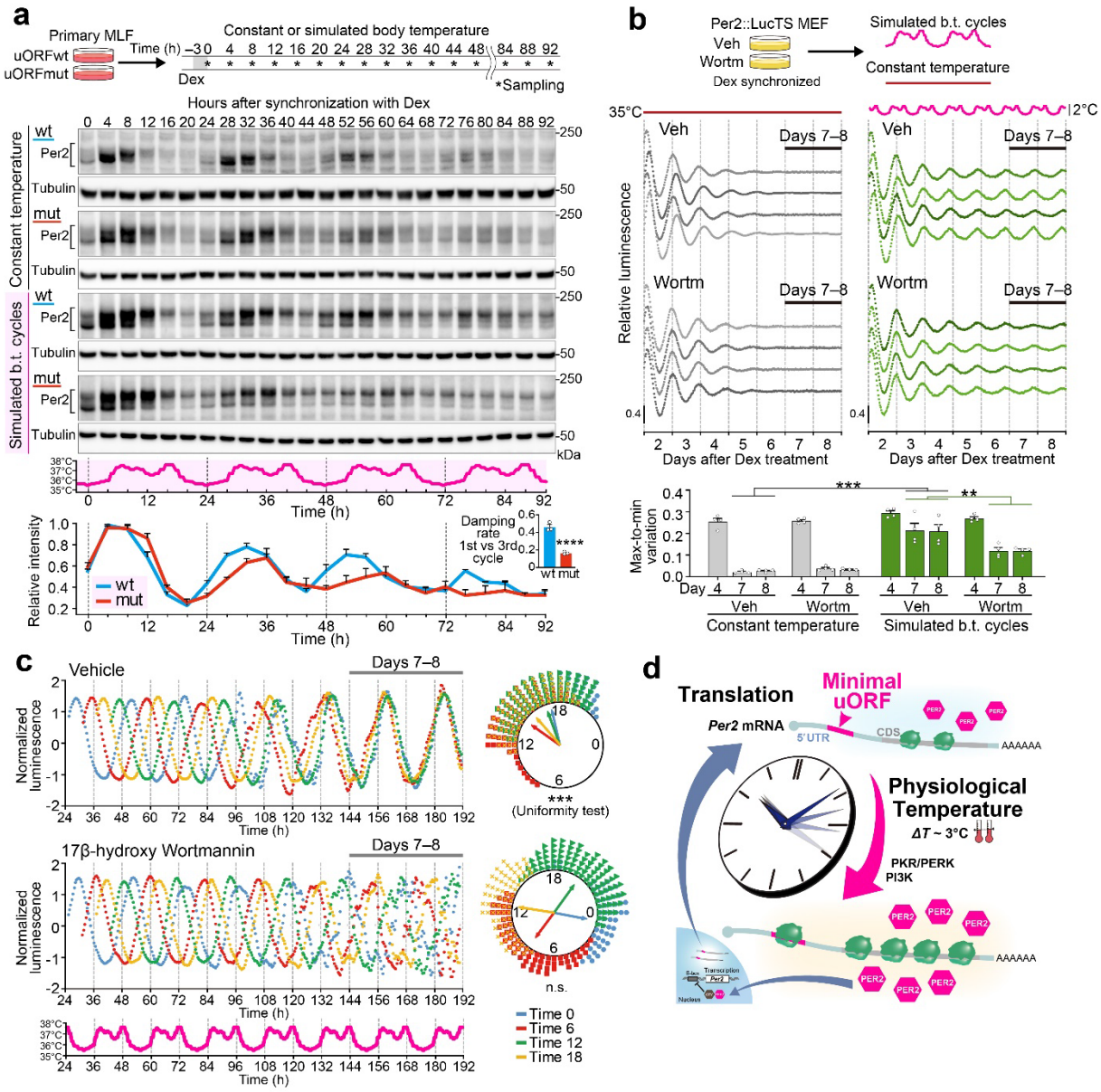
a
Primary MLF
uORFwt
uORFmut
Time (h)
Constant or simulated body temperature
Dex
*Sampling
Hours after synchronization with Dex
Constant temperature
Simulated b.t. cycles
wt
mut
Per2
Tubulin
kDa
Time (h)
Relative intensity
Damping rate 1st vs 3rd cycle
wt mut
b
Per2::LucTS MEF
Veh
Wortm
Dex synchronized
Simulated b.t. cycles
Constant temperature
35°C
12°C
Days 7–8
Relative luminescence
Days after Dex treatment
Max-to-min variation
Day
Constant temperature
Simulated b.t. cycles
c
Vehicle
17β-hydroxy Wortmannin
Normalized luminescence
Time (h)
(Uniformity test)
n.s.
Time 0
Time 6
Time 12
Time 18
d
Translation
Minimal uORF
Per2 mRNA
5'UTR
CDS
AAAAAA
Physiological Temperature
ΔT ~ 3°C
PKR/PERK
PI3K
PER2
Transcription
Per2
Nucleus

Figure 4 | *Per2* uORF is essential for circadian temperature entrainment. a, Temporal profiles of Per2 protein expression in WT and *Per2* uORF mutant MLFs with or without simulated body temperature cycles. Cells were sampled every 4 h over 4 consecutive days. Shown are representative immunoblots and normalized densitometry values ($n = 3$ biological replicates, mean ± s.e.m.). All immunoblot images are available in Supplementary Fig. 4. Inset bar graph shows the values of damping rate of the third cycle relative to the first cycle. ****$P < 0.0001$, unpaired two-sided Student's *t*-test. **b,** Temperature cycle-dependent circadian sustainability of Per2::LucTS cells in the presence or absence of 17β-hydroxy wortmannin. Cells were synchronized by Dex and released into either constant or fluctuating temperature conditions over 8 days. Raw data were detrended by 24-h moving average and expressed as relative to the first peak value of luminescence ($n = 4$, for each condition). The lower graphs show the values of daily max-to-min variance of days 4, 7, and 8. **$P = 0.0045$, on day 7, **$P = 0.0078$, on day 8, Veh vs. Wortm, ****$P < 0.0001$, simulated b.t. cycles vs. constant temperature, Three-way ANOVA followed by Tukey *post hoc* tests. **c,** Thermal entrainment of Per2::LucTS bioluminescence in the presence or absence of 17β-hydroxy wortmannin. Cells were synchronized by Dex every 6 h around the circadian cycle and released into a common simulated body temperature cycle. To emphasize the phase of rhythms, amplitudes were normalized using 24-h moving s.d. of the detrended luminescence. Rayleigh plots show phase distribution of the acrophase, which was defined as > 0.7 of the normalized amplitude, on days 7–8. Plots are color-coded according to the Dex-synchronizing time, each encoding the results of two biological replicates. Arrows in the circle are the Rayleigh plot vector. ***$P < 0.0001$, Uniformity test. n.s., not significant. **d,** A schematic drawing of the *Per2* uORF contributing to the circadian clock phase adaptation toward the physiological circadian body temperature cycle. Error bars indicate s.e.m.

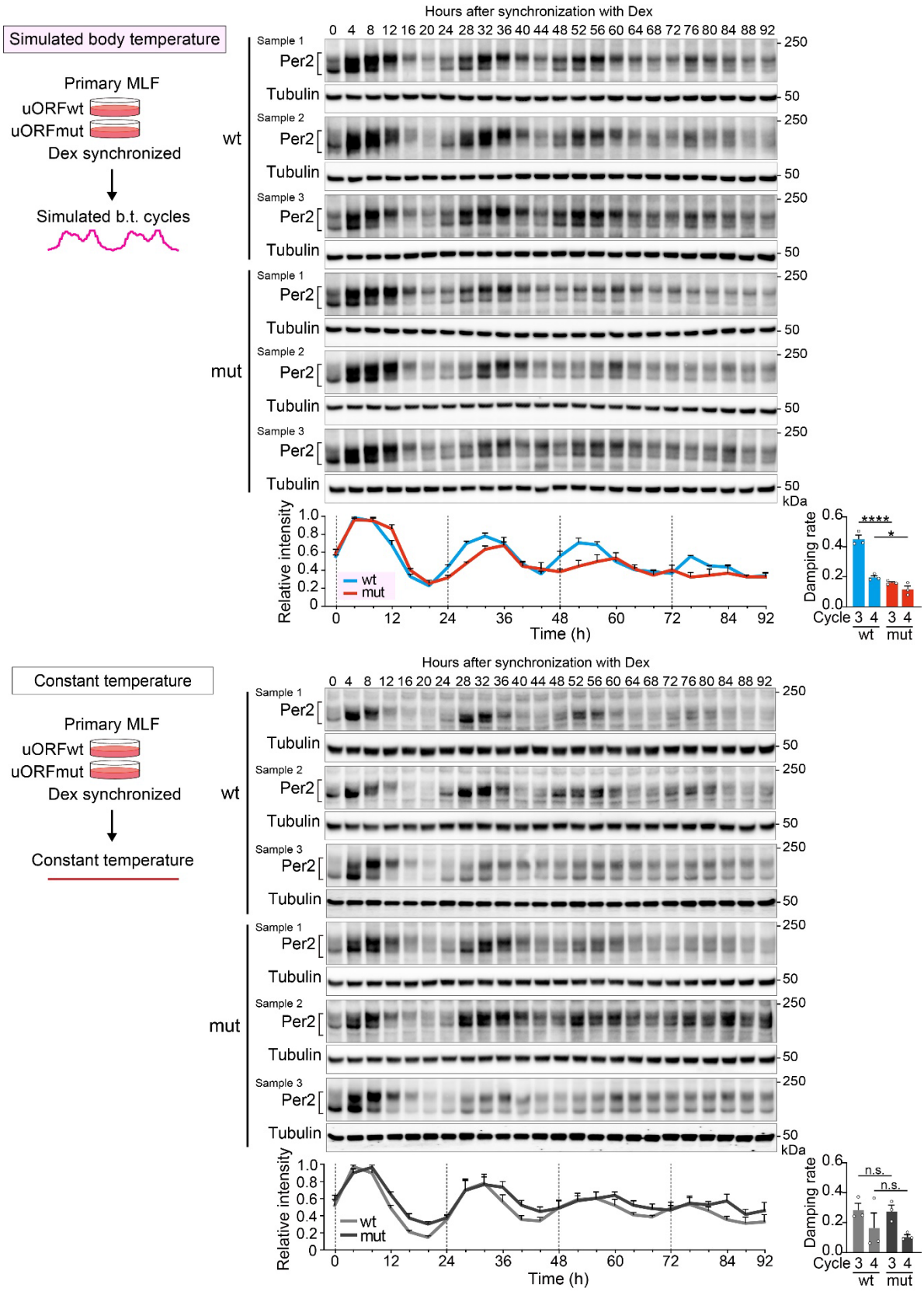
Simulated body temperature
Primary MLF
uORFwt
uORFmut
Dex synchronized
Simulated b.t. cycles
Hours after synchronization with Dex
0 4 8 12 16 20 24 28 32 36 40 44 48 52 56 60 64 68 72 76 80 84 88 92
wt
mut
Sample 1
Sample 2
Sample 3
Per2
Tubulin
250
50
kDa
Relative intensity
wt
mut
Time (h)
Damping rate
Cycle 3 4 3 4
wt mut
****
*
Constant temperature
Primary MLF
uORFwt
uORFmut
Dex synchronized
Constant temperature
Hours after synchronization with Dex
n.s.
n.s.

Supplementary Fig. 4 | Temporal profiles of Per2 protein expression in WT and *Per2* uORF mutant MLF cells with or without simulated body temperature cycles, related to Fig. 4a. Immunoblots of three biological replicates of Fig. 4a and their normalized densitometry values (mean ± s.e.m.) are shown. The blots of sample 1 are the same as Fig. 4a. Bar graphs show the values of damping rate of the third and fourth cycle relative to the first cycle. Error bars indicate s.e.m. ****$P < 0.0001$, *$P = 0.0381$.

Discussion

The ORF in the 5′ UTR is a post-transcriptional regulatory element considered to have undescribed roles in physiology[3, 4]. Here, I found a physiological role for uORF in a translation-dependent temperature entrainment mechanism of the circadian clock. A mild temperature change within a physiological range does not affect transcription but instead increase translation of *Per2* involving its uORF, identifying a new layer of regulation to the circadian clock entrainment (Fig. 4d).

The structure of AUG-stop minimal uORF of *Per2* is necessary for inducing WTS (warming temperature shift)-responsive translation, but its mechanism is completely unknown. Potential structural and functional difference between minimal and non-minimal uORFs might help to study the underlying mechanism required for Per2 regulation. Because of its minimal nature, no peptide is produced. The ribosomes were situated on the *Per2* uORF, with their P-site and A-site at the start and stop codon, respectively, representing the unique combinatory nature of initiation and termination codon. No ribosomal translocation occurs in this site, rendering no nascent peptide inside the ribosomal exit tunnel, a structure also unique to the minimal uORF. How these above features relate to Per2 WTS regulation is my next question, requiring further investigation. I noted that similar temperature-dependent ribosome accumulation occurs on the AUG-stop uORF sequences of other genes, such as *Drosha*, *Klf3*, and *Lgi4*, raising the

speculation that the minimal uORF might have a role in genes other than the Per2.

There are conceivable teleological benefits in having a translation-based control mechanism, alongst transcriptional regulation, to regulate expression of *Per2* in response to temperature. Firstly, *in vivo*, body temperature rises around the beginning of behaviorally active phase, which coincides with an increase in Per2 translation from its preexisting mRNA. Secondly and relatedly, because translation relies on mRNA abundance, for which *Per2* cycles robustly, WTS response of Per2 was highly phase-dependent, which is likely suitable for achieving phase-dependent phase entrainment. Thirdly, changes in physiological body temperature are continuous and gradual, thus translational regulation may serve as an adaptive and flexible base for changes in the Per2 protein level in response to body temperature. Lastly, having an additional layer of regulation, at the translation level, itself, may be advantageous in modulation of the transcription-translation-based circadian feedback loop.

My study revealed the existence of a translation-based circadian entrainment mechanism that is distinct from the canonical transcription-based circadian resetting mechanisms. Nevertheless, there are a number of limitations in my study. Firstly, the mechanism by which WTS promotes activation of PI3K remains unknown. It is possible to consider that some isozyme of PI3K itself could function as a thermosensitive enzyme. Temperature may also affect the fluidity of cellular membrane[33], thereby influencing the accessibility of PI3K to its substrate. Thermal

sensor(s) responsible for PI3K activation may also exist upstream, reminiscent of WTS-dependent activation of PERK/PKR. Secondly, the mechanism by which the *Per2* uORF mediates WTS response of *Per2* is still worth investigating. There are several possibilities: i) ribosomes may be poised at the *Per2* uORF for the initiation of the downstream CDS translation; ii) occupation of one of the two initiation codons by ribosome may increase the chance of ribosome entry to the non-occupied one, which in the *Per2* is the initiation codon of the CDS; iii) stalling ribosomes at the uORF may be able to recruit additional factor(s) to enhance the downstream CDS translation[34]. These possibilities will be examined in the future. Lastly, it is not known whether and how the minimal uORF-dependent thermal translational mechanism acts in concert with other known thermal clock-entrainment mechanisms, which include those involving HSF1[9-11] or Cirp[12]. Addressing how these transcriptional and post-transcriptional mechanisms coordinate to regulate thermal circadian entrainment will be the subject of my future studies.

Since the process of translation is evolutionarily conserved, the minimal uORF-mediated regulation of translation that I found in this study will be worth further testing in different species (e.g., fish, insects, nematode, and plants; all have minimal uORFs[35]) and in different biological contexts, including cancer biology, immunology, and neurosciences. Disturbance of the circadian clock has been linked to a variety of lifestyle-related diseases. My findings on the entrainment mechanism of the circadian clock may help to provide potential avenues for

therapeutic intervention of the circadian clock-related disorders.

References

1. Schwanhäusser, B. *et al.* Global quantification of mammalian gene expression control. *Nature* **473**, 337-342 (2011).
2. Tresenrider, A. *et al.* Integrated genomic analysis reveals key features of long undecoded transcript isoform-based gene repression. *Mol Cell* **81**, 2231-2245 e2211 (2021).
3. Chew, G.L., Pauli, A. & Schier, A.F. Conservation of uORF repressiveness and sequence features in mouse, human and zebrafish. *Nat Commun* **7**, 11663 (2016).
4. Johnstone, T.G., Bazzini, A.A. & Giraldez, A.J. Upstream ORFs are prevalent translational repressors in vertebrates. *EMBO J* **35**, 706-723 (2016).
5. Vattem, K.M. & Wek, R.C. Reinitiation involving upstream ORFs regulates ATF4 mRNA translation in mammalian cells. *Proc Natl Acad Sci U S A* **101**, 11269-11274 (2004).
6. Bollinger, T. & Schibler, U. Circadian rhythms - from genes to physiology and disease. *Swiss Med Wkly* **144**, w13984 (2014).
7. Logan, R.W. & McClung, C.A. Rhythms of life: circadian disruption and brain disorders across the lifespan. *Nat Rev Neurosci* **20**, 49-65 (2019).
8. Brown, S.A., Zumbrunn, G., Fleury-Olela, F., Preitner, N. & Schibler, U. Rhythms of mammalian body temperature can sustain peripheral circadian clocks. *Curr Biol* **12**, 1574-1583 (2002).
9. Saini, C., Morf, J., Stratmann, M., Gos, P. & Schibler, U. Simulated body temperature rhythms reveal the phase-shifting behavior and plasticity of mammalian circadian oscillators. *Genes Dev* **26**, 567-580 (2012).
10. Reinke, H. *et al.* Differential display of DNA-binding proteins reveals heat-shock factor 1 as a circadian transcription factor. *Genes Dev* **22**, 331-345 (2008).
11. Buhr, E.D., Yoo, S.H. & Takahashi, J.S. Temperature as a universal resetting cue for mammalian circadian oscillators. *Science* **330**, 379-385 (2010).
12. Morf, J. *et al.* Cold-inducible RNA-binding protein modulates circadian gene expression posttranscriptionally. *Science* **338**, 379-383 (2012).
13. Mito, M., Mishima, Y. & Iwasaki, S. Protocol for Disome Profiling to Survey Ribosome Collision in Humans and Zebrafish. *STAR Protoc* **1**, 100168 (2020).
14. Ingolia, N.T., Ghaemmaghami, S., Newman, J.R. & Weissman, J.S. Genome-wide analysis in vivo of translation with nucleotide resolution using ribosome profiling. *Science* **324**, 218-223 (2009).
15. Tisi, L.C. *et al.* Development of a thermostable firefly luciferase. *Analytica Chimica Acta* **457**, 115-123 (2002).
16. Doi, M. *et al.* Non-coding cis-element of Period2 is essential for maintaining organismal circadian behaviour and body temperature rhythmicity. *Nat Commun* **10**, 2563 (2019).

17. Doi, M. *et al.* Gpr176 is a Gz-linked orphan G-protein-coupled receptor that sets the pace of circadian behaviour. *Nat Commun* **7**, 10583 (2016).
18. Tainaka, M., Doi, M., Inoue, Y., Murai, I. & Okamura, H. Circadian PER2 protein oscillations do not persist in cycloheximide-treated mouse embryonic fibroblasts in culture. *Chronobiol Int* **35**, 132-136 (2018).
19. Morioka, S. *et al.* A mass spectrometric method for in-depth profiling of phosphoinositide regioisomers and their disease-associated regulation. *Nat Commun* **13**, 83 (2022).
20. Fustin, J.M. *et al.* RNA-methylation-dependent RNA processing controls the speed of the circadian clock. *Cell* **155**, 793-806 (2013).
21. Tamaru, T. *et al.* Synchronization of circadian Per2 rhythms and HSF1-BMAL1:CLOCK interaction in mouse fibroblasts after short-term heat shock pulse. *PLoS One* **6**, e24521 (2011).
22. Koyanagi, S. *et al.* cAMP-response element (CRE)-mediated transcription by activating transcription factor-4 (ATF4) is essential for circadian expression of the Period2 gene. *J Biol Chem* **286**, 32416-32423 (2011).
23. Gerber, A. *et al.* Blood-borne circadian signal stimulates daily oscillations in actin dynamics and SRF activity. *Cell* **152**, 492-503 (2013).
24. Sato, S., Fujita, N. & Tsuruo, T. Modulation of Akt kinase activity by binding to Hsp90. *Proc Natl Acad Sci U S A* **97**, 10832-10837 (2000).
25. Oehler-Jänne, C. *et al.* Temperature sensitivity of phospho-Ser(473)-PKB/AKT. *Biochem Biophys Res Commun* **375**, 399-404 (2008).
26. Yoshihara, T. *et al.* Heat stress activates the Akt/mTOR signalling pathway in rat skeletal muscle. *Acta Physiol (Oxf)* **207**, 416-426 (2013).
27. Kitani, S. *et al.* Inhibition of IgE-mediated histamine release by myosin light chain kinase inhibitors. *Biochem Biophys Res Commun* **183**, 48-54 (1992).
28. Hausdorff, S.F. *et al.* Identification of wortmannin-sensitive targets in 3T3-L1 adipocytes. DissociationoOf insulin-stimulated glucose uptake and glut4 translocation. *J Biol Chem* **274**, 24677-24684 (1999).
29. Hennessy, B.T., Smith, D.L., Ram, P.T., Lu, Y. & Mills, G.B. Exploiting the PI3K/AKT pathway for cancer drug discovery. *Nat Rev Drug Discov* **4**, 988-1004 (2005).
30. Crosby, P. *et al.* Insulin/IGF-1 Drives PERIOD Synthesis to Entrain Circadian Rhythms with Feeding Time. *Cell* **177**, 896-909 e820 (2019).
31. Zhou, J. *et al.* Dynamic m(6)A mRNA methylation directs translational control of heat shock response. *Nature* **526**, 591-594 (2015).
32. Goda, T. *et al.* Calcitonin receptors are ancient modulators for rhythms of preferential temperature in insects and body temperature in mammals. *Genes Dev* **32**, 140-155 (2018).
33. Murata, N. & Los, D.A. Membrane Fluidity and Temperature Perception. *Plant*

Physiol **115**, 875-879 (1997).
34. Shu, X.E., Mao, Y., Jia, L. & Qian, S.B. Dynamic eIF3a O-GlcNAcylation controls translation reinitiation during nutrient stress. *Nat Chem Biol* (2021).
35. Tanaka, M. *et al.* The Minimum Open Reading Frame, AUG-Stop, Induces Boron-Dependent Ribosome Stalling and mRNA Degradation. *Plant Cell* **28**, 2830-2849 (2016).

Acknowledgements

First of all, I wish to express sincere thanks to Prof. Masao Doi and Dr. Takahito Miyake, for their direction and kind encouragement throughout my graduated study.

I am grateful to all the member of Doi's lab for their advice and help. In particular, I appreciate the technical assistance and contributions of Ms. Xinyan Shao and Mr. Yuto Aoki.

I thank my parents for their support and encouragement. Without their support I would not have accomplished this thesis.